CNWRA **A center of excellence in earth sciences and engineering**

A Division of Southwest Research Institute™
6220 Culebra Road • San Antonio, Texas, U.S.A. 78228-5166
(210) 522-5160 • Fax (210) 522-5155

June 4, 2001
Contract No. NRC–02–97–009
Account No. 20.01402.471

U.S. Nuclear Regulatory Commission
ATTN: Mrs. Deborah A. DeMarco
Office of Nuclear Material Safety and Safeguards
TWFN Mail Stop 8 A23
Washington, DC 20555

Subject: Submittal of Poster—The Geometric Strength of Fault Systems

Dear Mrs. DeMarco:

The additional posters that were not shipped last week are included in this mailing. The poster is for a presentation at the American Association of Petroleum Geologists (AAPG) 2001 National Meeting. It is based on work done by David Ferrill, Darrell Sims, and John Stamatakos of the CNWRA. The poster describes the CNWRA's analysis of potential fault movement using 3DStress™. The abstract for the poster, The Geometric Strength of Fault Systems, was approved by NRC in an e-mail from P. Justus on November 2, 2000. This poster will be presented at the AAPG National Meeting on June 5, 2001.

If you have any questions please contact Dr. David Ferrill at 210-522-6082 or me at 210-522-5252.

Sincerely,

Budhi Sagar
Technical Director

rae

Attachment

cc:	J. Linehan	B. Meehan	S. Wastler	W. Patrick	D. Sims
	W. Reamer	J. Greeves	T. Essig	CNWRA Dirs/EMs	J. Stamatakos
	B. Leslie	J. Piccone	P. Justus	D. Ferrill	T. Nagy (SwRI Contracts)
	E. Whitt				

D:\GLGP Group\letters\sds\poster2-06-2001bs.wpd

THE GEOMETRIC STRENGTH OF FAULT SYSTEMS

David A. Ferrill[1], Alan P. Morris[2], Darrell W. Sims[1], and John A. Stamatakos[1]
[1]Center for Nuclear Waste Regulatory Analyses, Southwest Research Institute, 6220 Culebra Road, San Antonio, Texas 78238-5166
[2]Department of Earth and Environmental Science, University of Texas at San Antonio, San Antonio, Texas 78249-0663

ABSTRACT

Faults optimally oriented for slip within an ambient stress field are geometrically weak compared with other fault orientations. Evolving fault systems undergo changes that lead to both geometric strengthening and weakening of faults. Given a single stress regime, geometrically weak faults grow and accumulate displacement, and geometrically strong faults tend to be abandoned. This natural selection process results in a well-organized fault pattern that reflects the evolution of the stress field. Initial fault surfaces are often en echelon and not connected. These faults grow by segment nucleation, growth, and connection by curved propagation or connecting fault formation. Fault propagation prior to linkage produces local perturbations in the stress field that modify continuing fault propagation. As fault segments link, local stress field perturbations are relieved and certain fault segments become geometrically stronger in the ambient stress field. These poorly oriented fault segments are bypassed by newly formed cutoff faults that straighten the overall fault surface. This process results in an active fault surface that is smoother, geometrically weaker, and with a smaller surface area. In addition, slip on an imbricate system of normal faults progressively reorients fault planes to shallower and less favorable dips, eventually causing the initiation of new, more favorably oriented faults. Analyses of natural fault systems from the Basin and Range Province illustrate this fault system evolution.

INTRODUCTION

(1) A fault that is favorably-oriented in the stress field to accommodate slip (i.e., has high slip tendency) is geometrically weak.

(2) Natural fault systems initiate with orientations that are variable but which cluster around the optimal orientations determined by stress field and rock characteristics - optimal orientations may not necessarily form simple conjugate sets.

(3) Fault orientations that differ from the ideal result from:

- *fault interaction*
- *reactivation of pre-existing fabrics (e.g., joints, basement faults)*
- *fault and fault block rotation*
- *stress system evolution.*

(4) Fault linkage and growth leads to abandonment of unfavorably oriented fault (geometrically strong) segments.

(5) In relatively simple stress fields, fault orientation patterns provide a good indication of regional stress field - which is the basis for classical fault analysis.

FAULT SYSTEMS IN THE VOLCANIC TABLELAND

Figure 1.

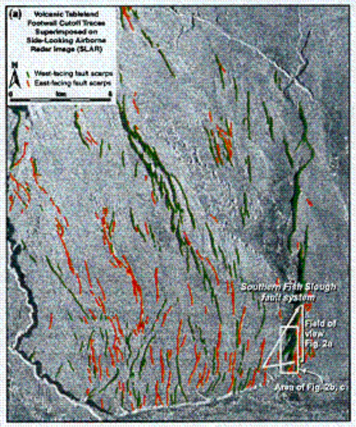

Figure 1. Fault trace maps of the Volcanic Tableland, north of the town of Bishop in the Owens Valley, California.

(a) Fault traces interpreted on side-looking airborne radar image. Radar illumination was from the east, therefore west-facing fault scarps cast shadows and east-facing scarps appear bright. Only footwall traces (red for east-facing, green for west-facing) are shown for clarity and accuracy - because of the shadow effect the hanging wall traces of down-to the west normal faults are obscured.

(b) Footwall traces color-coded according to slip tendency (Morris et al., 1996) for the stress field:
σ_1 = vertical
σ_2 = horizontal, azimuth 175°, 50% of σ_1
σ_3 = horizontal, azimuth 265°, 30% of σ_1
Color-code scale is given in inset (ii).

Inset (i) Rose diagram. Petals are cumulative fault segment length in 10° azimuth bins, color-coded by slip tendency. Points are maximum continuous fault segment length for each azimuth bin.

Inset (ii) Lower hemisphere, equal angle projection of

The Volcanic Tableland north of Bishop California is formed by the welded unit of the 738,000 year old Bishop tuff (Izett et al., 1988). More than 500 normal faults with displacements in excess of 1 meter cut the tuff. The arid climate and weathering-resistant tuff combine to preserve well-exposed fault-line scarps (Pinter, 1995). Slip tendency analysis indicates that the orientations of approximately 90% of the faults are consistent with EW extension.

Faults in the Volcanic Tableland exhibit a range of interactions. Features include:

- *en echelon arrays*
- *relay ramps*
- *linked faults*

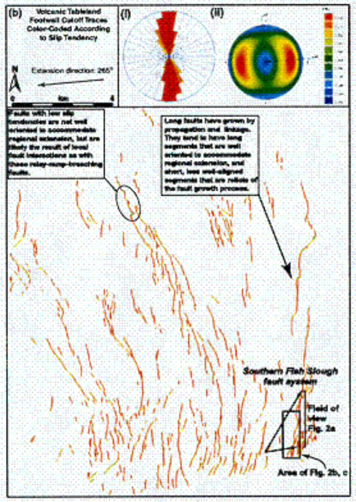

Longer faults, resulting from fault propagation and linkage, are better oriented to accommodate the EW regional extension than shorter faults.

Figure 2.

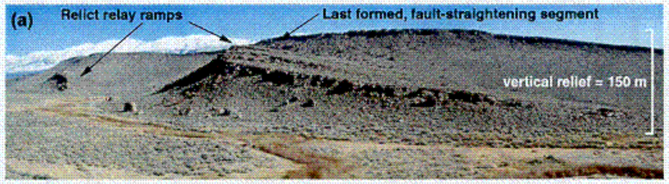

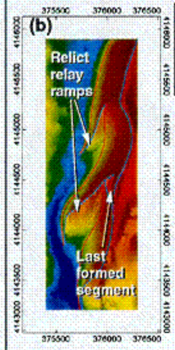

Figure 2. The southern Fish Slough fault system, for location see Fig. 1.

(a) Photograph showing the two detached relay ramps in the hanging wall of the Fish Slough fault.

(b) High resolution GPS map of southern Fish Slough fault system.

(c) Developmental sequence of en echelon fault array into the through-going Fish Slough fault.

The southern end of the Fish Slough fault system illustrates the development of a through-going fault from an array of three en echelon faults (Ferrill et al., 1999):
(1) Faults initially separate and variable in orientation.
(2) Fault growth and linkage led to the abandonment of original fault tips.
(3) Fault segments that are unfavorably oriented to accommodate EW extension are superseded by more favorably oriented (geometrically weaker) fault segments that effectively shorten and straighten the fault.

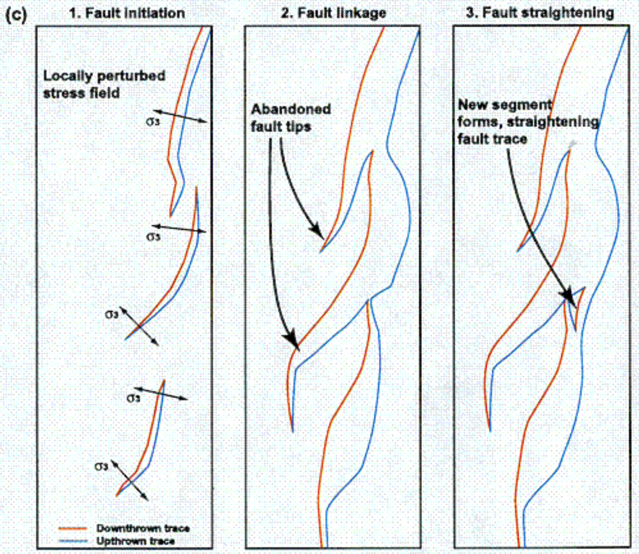

C01

THE GEOMETRIC STRENGTH OF FAULT SYSTEMS

David A. Ferrill[1], Alan P. Morris[2], Darrell W. Sims[1], and John A. Stamatakos[1]
[1]Center for Nuclear Waste Regulatory Analyses, Southwest Research Institute, 6220 Culebra Road, San Antonio, Texas 78238-5166
[2]Department of Earth and Environmental Science, University of Texas at San Antonio, San Antonio, Texas 78249-0663

ROTATION OF NORMAL FAULTS

Figure 3.

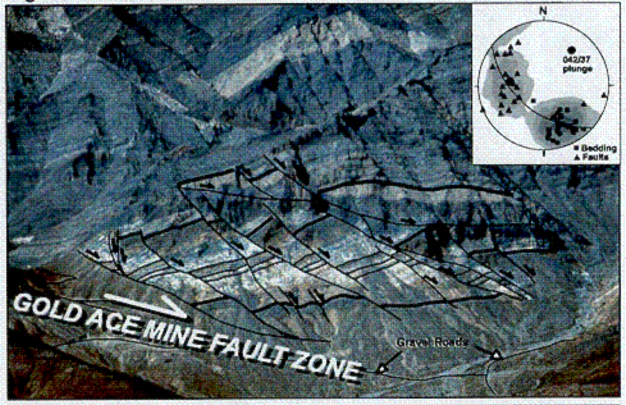

Figure 3. The Gold Ace Mine fault system, Bare Mountain, Nevada.
Interpreted oblique aerial photograph of the normal fault system developed in the hanging wall of the Gold Ace Mine fault exposed in the southwestern flank of Bare Mountain, Nevada. The direction of view is down structural plunge (i.e., parallel to the bedding cutoff lines in the fault planes). The inset is a lower hemisphere, equal area projection of the principal structural elements of the exposure.

In imbricate fault systems faults rotate during slip. This rotation re-orients overlying faults so that they become less favorably oriented to accommodate slip (e.g., Lister & Davis, 1986). Geometrically weak faults may become geometrically stronger. This is the case in the hanging wall of the Gold Ace Mine fault, where continuous slip has rotated faults into orientations that are no longer favorable for slip.

Figure 4.

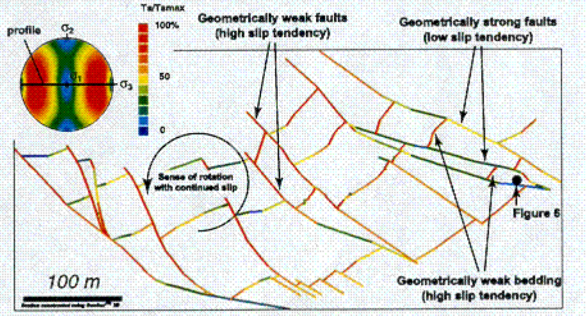

Figure 4. Slip tendency analysis of the fault system illustrated above (Fig. 3) projected onto a plunge-perpendicular cross-section plane. The modeled stress system is: σ_1 = 90MPa, σ_2 = 65 MPa, σ_3 = 25 MPa (Ferrill et al., 1998).

Figure 5.

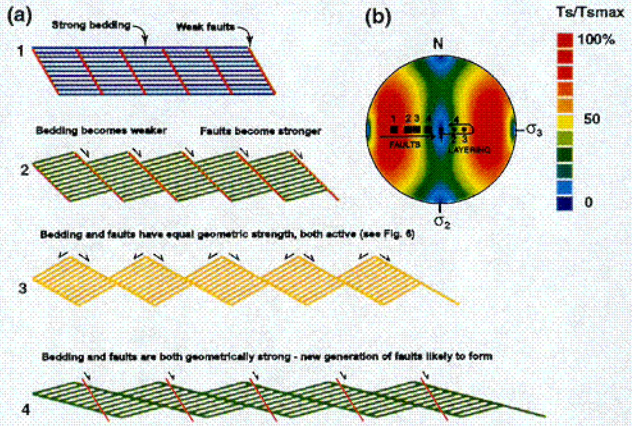

Figure 5. Slip tendency analysis of imbricate normal faults and layering during progressive extension.

(a) Schematic cross-sections through progressive extension sequence.

(b) Lower hemisphere equal-angle projection illustrating slip tendency distribution for faults in a typical extensional stress regime. Conceptual rotation paths of faults and layering within the stress field during progressive deformation are also shown.

(1) Faults initiate with ideal orientations for slip, bedding has the worst orientation for slip.

(2) Faults rotate to worse orientations for slip, bedding rotates to a better orientation for slip.

(3) At some point both bedding and faults become active slip surfaces.

(4) Bedding and fault surfaces rotate to unfavorable orientations and new faults form.

At Bare Mountain there is abundant evidence for steps 1 through 3 above. Figure 6a shows the slip systems at a location where fault block rotation has re-oriented faults into geometrically strong configurations whereas the bedding has attained a dip that permits slip.

The field photograph and interpretation in Figure 6b show the offset of the dolomitic (brown) beds by faulting, followed by slip along bedding planes cutting the earlier faults. This in turn is followed by reactivated slip along the earlier fault surfaces.

Figure 6.

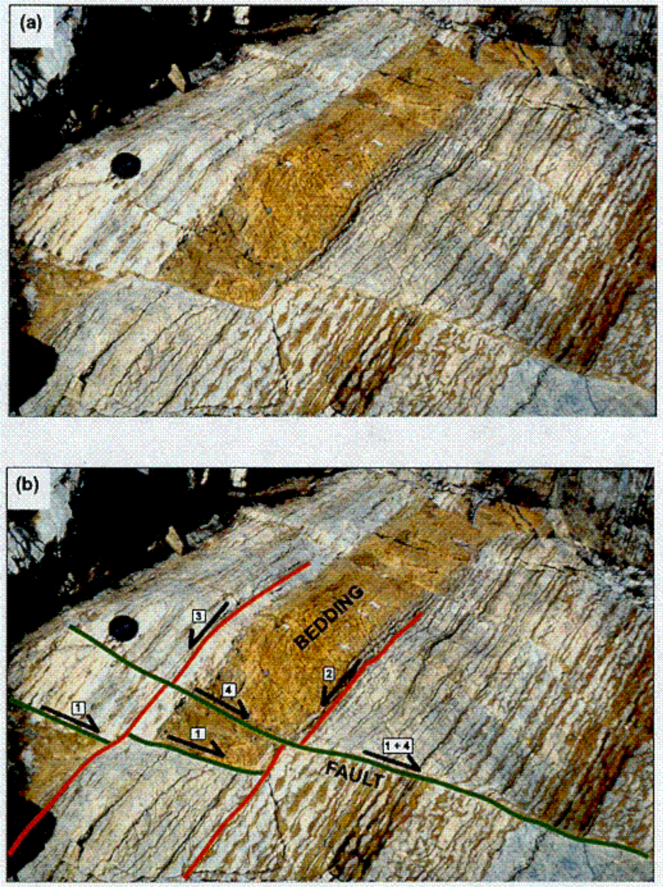

Figure 6. Early high-angle faults cut by bedding-parallel faults (Ferrill et al., 2000).

(a) Uninterpreted field photograph of faulted bedding in carbonate rocks within the hanging wall of the Gold Ace Mine fault. Lens cap for scale, location shown in Figure 4.

(b) Simplified interpretation of (a). High angle fault 1, in green, displaces bedding. This is followed by slip on bedding-parallel faults 2 and 3 which displaces fault 1. Finally slip on fault 4 displaces 2 and 3 and increases the total displacement on the continuation of fault 1 to the lower right.

C02

THE GEOMETRIC STRENGTH OF FAULT SYSTEMS

David A. Ferrill[1], Alan P. Morris[2], Darrell W. Sims[1], and John A. Stamatakos[1]
[1]Center for Nuclear Waste Regulatory Analyses, Southwest Research Institute, 6220 Culebra Road, San Antonio, Texas 78238-5166
[2]Department of Earth and Environmental Science, University of Texas at San Antonio, San Antonio, Texas 78249-0663

CONTRACTIONAL FAULTS

Figure 7.

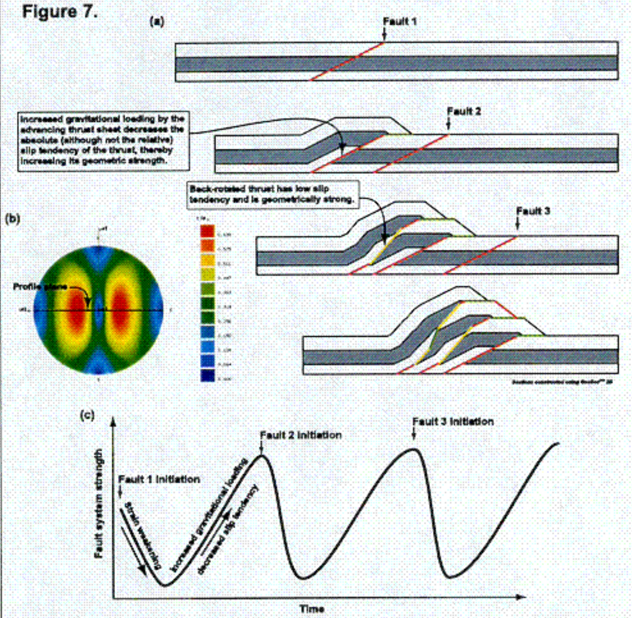

Figure 7. Development of a classic "break-forward" imbricate thrust stack.

(a) The thrust faults are color-coded according to slip tendency within the stress system:
σ_1 = horizontal azimuth 270
σ_2 = horizontal azimuth 180, 50% of σ_1
σ_3 = vertical, 30% of σ_1

(b) Lower hemisphere, equal angle stereographic projection of poles to all surfaces color-coded by slip tendency.

(c) Schematic graph of time versus fault system strength.

During the development of a break-forward imbricate thrust system, each thrust fault experiences the following developmental sequence:

- fault initiation along a favorably oriented trajectory

- fault slip and strain weakening

- as the hanging wall rises there is an increase in gravitational loading of the thrust surface, which decreases the absolute slip tendency of the fault and hence increases its geometric strength

- initiation of another fault in the unloaded footwall ahead of the toe of the advancing thrust system causes back-rotation of the earlier fault to a less favorable orientation for further slip.

STRIKE-SLIP FAULTS

Figure 8.

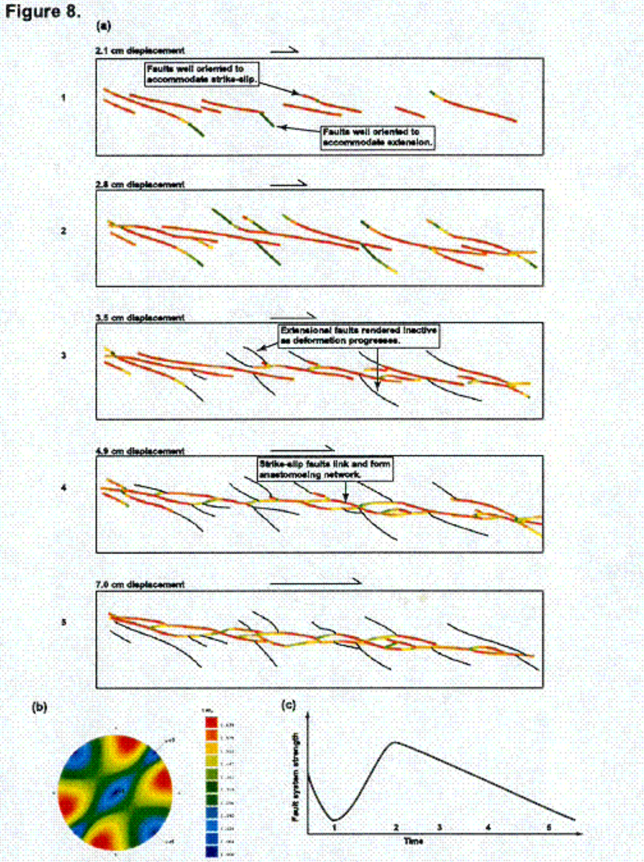

Figure 8. Development of a strike-slip fault system (from Naylor et al., 1986).

(a) Plan views of developing strike-slip system in sandbox model. Fault traces are color-coded by slip tendency, black traces are inactive.

(b) Lower hemisphere, equal angle projection of poles to all surfaces color-coded by slip tendency.

(c) Schematic graph of time versus fault system strength.

Initially, faults with a variety of orientations develop. As total displacement increases and faults grow and link, the less well-oriented fault segments are abandoned and the geometrically weaker faults increase in length.

SUMMARY

(1) The geometric strength of a fault is primarily a function of its slip tendency within the ambient stress field.

(2) Natural fault systems initially form with a spectrum of active slip orientations resulting from:

- *fault interaction*
- *reactivation of pre-existing fabrics*
- *fault rotation*
- *stress system evolution.*

(3) As a fault system evolves, linkage and growth lead to abandonment of geometrically strong fault segments.

(4) An important corollary of this sequence of development is that the majority of faults provide a good representation of the overall stress field that existed at the time of their formation.

REFERENCES

Ferrill, D.A., Morris, A.P., Stamatakos, J.A., Jones, S.M., 1998, Extensional layer-parallel shear and normal faulting: Journal of Structural Geology, v. 20, p. 355-362.

Ferrill, D.A., Morris, A.P., Stamatakos, J.A., Sims, D.W., 2000, Crossing conjugate normal faults: American Association of Petroleum Geologists Bulletin, v. 84, p. 1543-1559.

Ferrill, D.A., Stamatakos, J.A., Sims, D.W., 1999, Normal fault corrugation: implications for growth and seismicity of active normal faults: Journal of Structural Geology, v. 21, p. 1027-1038.

Izett, G.A., Obradovich, J.D., Mehnert, H.H., 1988, The Bishop ash bed (middle Pleistocene) and some older (Pliocene and Pleistocene) chemically and mineralogically similar ash beds in California, Nevada, and Utah: U.S. Geological Survey Bulletin 1675, 38p.

Lister, G.S., Davis, G.A., 1989, The origin of metamorphic core complexes and detachment faults formed during Tertiary continental extension in the northern Colorado River region, U.S.A.: Journal of Structural Geology, v. 11, p. 65-94.

Morris, A.P., Ferrill, D.A., Henderson, D.B., 1996, Slip tendency analysis and fault reactivation: Geology, v. 24, p.275-278.

Naylor, M.A., Mandl, G. Sijpesteijn, C.H.K., 1986, Fault geometries in basement-induced wrench faulting under different initial stress states: Journal of Structural Geology, v. 7, p. 737-752.

Pinter, N., 1995, Faulting on the Volcanic Tableland, Owens Valley, California: The Journal of Geology, v. 103, p. 73-83.

ACKNOWLEDGMENTS

This work was supported by the U.S. Nuclear Regulatory Commission (NRC, contract number NRC-02-97-009). This is an independent product of the Center for Nuclear Waste Regulatory Analyses (CNWRA) and does not necessarily reflect the views or regulatory position of the NRC. We thank Nick Davatzes for geo-referencing of the side-looking airborne radar image of the Volcanic Tableland and for his contributions to the interpretation of the fault traces thereon. Peter LaFemina, Ron Martin, and Laura Conner provided invaluable field assistance during the GPS mapping of the southern Fish Slough fault system, and Deborah Waiting assisted with the production of figures. We also thank Larry McKague and Budhi Sagar for helpful reviews of this work.

C03